



Published in final edited form as:

*J Neurointerv Surg.* 2021 July ; 13(7): 642–646. doi:10.1136/neurintsurg-2020-016601.

## Hemodynamics in Aneurysm Blebs with Different Wall Characteristics

Seyedeh Fatemeh Salimi Ashkezari<sup>1</sup>, Fernando Mut<sup>1</sup>, Bong Jae Chung<sup>2</sup>, Alexander K. Yu<sup>3</sup>, Christopher J. Stapleton<sup>4</sup>, Alfred P. See<sup>5</sup>, Sepideh Amin-Hanjani<sup>5</sup>, Fady T. Charbel<sup>5</sup>, Behnam Rezai Jahromi<sup>6</sup>, Mika Niemelä<sup>6</sup>, Juhana Frösen<sup>7</sup>, Spandan Maiti<sup>8</sup>, Anne M. Robertson<sup>8,9</sup>, Juan R. Cebal<sup>1,10</sup>

<sup>1</sup>Department of Bioengineering, George Mason University, Fairfax, VA, USA <sup>2</sup>Department of Mathematical Sciences, Montclair State University, Montclair, NJ, USA <sup>3</sup>Neurosurgery, Allegheny General Hospital, Pittsburgh, PA, USA <sup>4</sup>Neurosurgery, Massachusetts General Hospital, Boston, MA, USA <sup>5</sup>Department of Neurosurgery, University of Illinois at Chicago, Chicago, IL, USA <sup>6</sup>Neurosurgery Research Group, Biomedicum Helsinki, University of Helsinki, Helsinki, Finland <sup>7</sup>Department of Neurosurgery, University of Tampere and Tampere University Hospital, Tampere, Finland <sup>8</sup>Department of Mechanical Engineering and Material Science, University of Pittsburgh, Pittsburgh, PA, USA <sup>9</sup>Department of Bioengineering, University of Pittsburgh, Pittsburgh, PA, USA <sup>10</sup>Department of Mechanical Engineering, George Mason University, Fairfax, VA, USA

### Abstract

**Background**—Blebs are important secondary structures of intracranial aneurysms (IA) associated with increased rupture risk and can affect local wall stress and hemodynamics. Mechanisms of bleb development and evolution are not clearly understood. We investigate the relationship between blebs with different wall characteristics and local hemodynamics and rupture sites.

**Methods**—Blebs with different wall appearances in intra-operative videos were analyzed with image-based computational fluid dynamics. Thin red blebs were compared against thick

---

**Corresponding Author:** Seyedeh Fatemeh Salimi Ashkezari, ssalimia@gmu.edu, +1(720)369-6390, Bioengineering Department, Volgenau School of Engineering, George Mason University, 4400 University Drive, Fairfax, VA 22030, USA.

#### Contributorship Statement

S.F.S.A., J.F., S.M., A.M.R., and J.R.C. designed the study. A.K.Y., C.J.S., A.P.S., S.A.H., F.T.C., B.R.J., M.N., and J.F. contributed to data collection. F.M. contributed to development of methodology. F.M. and J.R.C. designed the software tools. B.J.C. simulated vascular reconstructions. S.F.S.A. and J.R.C. identified blebs in the dataset. S.F.S.A. curated the data. S.F.S.A. and J.R.C. performed the data analysis. S.F.S.A., F.M., A.M.R., and J.R.C. contributed to the interpretation of the results. A.M.R. and J.R.C. acquired funding, supervised students, and coordinated the project. S.F.S.A. and J.R.C. drafted the manuscript. All authors contributed to manuscript edition and approved the final manuscript.

#### Competing Interests

None declared.

#### Data Availability

The data that support the findings of this study are available from the corresponding author, upon request.

#### Research Ethics Approval

The protocols for patient consent, handling of patient data and analysis were approved by the institutional review board (IRBs) at the University of Pittsburgh (Protocol # STUDY20020015), University of Illinois at Chicago (Protocol # 2015-0322), Allegheny General Hospital (Protocol # RC-5141), and Helsinki University Hospital. The whole study's IRB is overseen by the University of Pittsburgh's IRB.

atherosclerotic/hyperplastic white/yellow blebs. Rupture points were identified in videos of ruptured aneurysms harboring blebs.

**Results**—Thin blebs tended to be closer to the inflow than atherosclerotic blebs of the same aneurysm ( $p=0.0234$ ). Blebs near the inflow had higher velocity ( $p=0.0213$ ), vorticity ( $p=0.0057$ ), shear strain rate ( $p=0.0084$ ), wall shear stress (WSS,  $p=0.0085$ ), and WSS gradient ( $p=0.0151$ ) than blebs far from the inflow. In a subset of 12 ruptured aneurysms harboring blebs, rupture points were associated with thin blebs in 42% of aneurysms, atherosclerotic blebs in 25%, and were away from blebs in the remaining 33%.

**Conclusions**—Not all blebs are equal, some have thin translucent walls while others have thick atherosclerotic walls. Thin blebs tend to be located closer to the inflow than atherosclerotic blebs. Blebs near the inflow are exposed to stronger flows with higher and spatially variable WSS than blebs far from the inflow which tend to have uniformly lower WSS. Aneurysms can rupture at thin blebs, atherosclerotic blebs, and even away from blebs. Further study of wall failure in aneurysms with different blebs types is needed.

---

## Introduction

Many intracranial aneurysms (IAs) have well defined sub-structures or daughter sacs known as blebs.<sup>1</sup> The presence of blebs is considered a risk factor for rupture<sup>2</sup> and is one of the few aneurysm-specific factors used in aneurysm scoring scales.<sup>3-5</sup> Since blebs can have an effect on the wall stress as well as the local hemodynamics, they have recently gained increasing interest. Moreover, vessel wall imaging and detection of small localized aneurysm enlargement are being investigated as potential means of assessing aneurysm instability.<sup>6,7</sup> Blebs are thought to be a consequence of focal weakening of the aneurysm wall.<sup>2,8</sup> However, the mechanisms responsible for their development and evolution are not clearly understood. Furthermore, it is not clear how they influence aneurysm rupture.

Previous studies have shown that aneurysm walls can be highly heterogeneous. They can have thin translucent regions or thick atherosclerotic walls.<sup>9,10</sup> They can have collagen fiber distributions with unidirectional or bidirectional orientations, and thick wavy fibers or thin fragmented fibers.<sup>11</sup> Aneurysm walls may contain micro and macro calcifications and lipid pools.<sup>12</sup> All of these structural characteristics can affect the strength of the wall and the distribution of intramural stresses.<sup>11</sup> On the other hand, hemodynamics is thought to play an important role in the mechanisms responsible for the local changes and remodeling of the wall that may lead to some of these structural characteristics.<sup>13</sup> Likewise, hemodynamics is thought to be an important factor in the development of aneurysm blebs.<sup>14,15</sup>

The current study investigates the relationship between aneurysm blebs with different structural characteristics and their local hemodynamic environment, as well as their relationship to aneurysm rupture sites.

## Methods

### Data

A total of 97 intracranial aneurysms harboring blebs treated with microsurgical clipping were selected from our database.<sup>1</sup> Blebs have been visually identified and interactively marked for all aneurysms in this database (97 aneurysms with 122 blebs, 173 without blebs), as previously reported.<sup>1</sup> All these aneurysms were imaged prior to surgery with 3D rotational angiography (3DRA) or computed tomographic angiography (CTA). For a subset of 32 aneurysms harboring 41 blebs intra-operative videos, where the blebs were visible, were also available. For this study, deidentified vascular geometries and intra-operative videos were obtained from our database. More details about patient and aneurysm characteristics are presented in Supplementary Table I.

### Flow Modeling

Patient-specific vascular models were reconstructed from 3D images as previously described,<sup>16</sup> and blebs were marked on these models<sup>1</sup> (see Fig. 1a–c). Pulsatile computational fluid dynamics (CFD) simulations were carried out by numerically solving the Navier-Stokes equations with in-house software.<sup>17</sup> Inflow boundary conditions were prescribed at the internal carotid or vertebral arteries by scaling representative waveforms with an empirical power-law relating flow rate and vessel diameter, derived from in-vivo measurements.<sup>18</sup> Outflow boundary conditions were imposed to satisfy Murray's law. Simulations were performed for two cardiac cycles with a timestep of 0.01 sec. As in a previous study,<sup>19</sup> a second CFD model was automatically constructed by virtually removing the bleb(s) to approximate the flow conditions in each aneurysm prior to the formation of the bleb(s) (Fig. 1d).

### Bleb Hemodynamics

The blebs identified in each aneurysm were characterized by computing several variables related to: 1) strength of the flow stream within the bleb, 2) distribution (magnitude, heterogeneity, oscillations) of the wall shear stress (WSS) distribution over the bleb surface, and 3) location of the bleb relative to the inflow stream and on the aneurysm sac. A summary of these variables is presented in Supplementary Table II. Hemodynamic variables were computed using the same tools and techniques previously used to characterize the hemodynamics in the entire aneurysm.<sup>20</sup>

In order to characterize the local hemodynamic conditions at bleb sites prior to their formation, the bleb regions were first projected to the model with virtually removed blebs (Fig. 1d), and then hemodynamic variables were calculated over these regions.

### Bleb Location

Bleb location relative to the inflow stream (DINF, Supplementary Table II) was computed as follows. For each bleb region in the model with deleted blebs, a set of close-by streamlines was computed. For this purpose, seed points were randomly selected in the proximity of the region and streamlines that pass through these seeds and extend to the aneurysm inflow and outflow were computed. For each of these streamlines, the length along the path from the

inflow to the seed, and from the seed to the outflow were computed. The ratio of the distance to the inflow over the distance to the outflow was computed and given as a percentage. The location of the region was then given as the average of the distance to the inflow over several (10) such streamlines. The process is illustrated in Fig. 1d–f.

Bleb location on the aneurysm sac was characterized as follows. As in previous studies,<sup>1</sup> the aneurysm neck was first interactively delineated on the vascular model (Fig. 1g), then the sac was subdivided into three non-overlapping regions corresponding to the neck, body, or dome according to the geodesic distance to the neck line (neck region=0–20% of maximum geodesic distance to neck, body region=20–60% of maximum geodesic distance to neck, and dome region=60–100% of maximum geodesic distance to neck) (Fig. 1h). The location of the bleb was then assigned to the neck, body, or dome depending on the maximum overlap of its area and each of these three aneurysm regions (Fig. 1i).

### Bleb Walls

Intra-operative videos were inspected to characterize bleb walls. Once the aneurysm was exposed, and prior to clipping, the surgical orientation was inferred by observing the aneurysm and the connected vessels. Next, blebs that had been previously marked on the 3D vascular models were visually identified in the intra-operative videos. Then, 41 blebs were classified as: 1) “thin” translucent walls as those with a red appearance, 2) “atherosclerotic” walls as those with a white (hyperplastic) or yellow (fatty) appearance, or 3) “unremarkable” walls as those with a pinkish coloration similar to normal arteries.<sup>10</sup> Another 8 blebs could not be observed in the available videos (not exposed during the surgical procedure), and were not considered for this part of the study. Additionally, when possible (i.e. visible in the videos), rupture sites were identified in ruptured aneurysms harboring blebs. Rupture points were visible as a hole in the wall or a hematoma attached to the rupture site.<sup>10</sup> These features usually have a different visual appearance (small tears, dark thrombus) than thin (translucent, red) or atherosclerotic walls (opaque, thick white / yellow walls) (see Supplementary Figures III–VI).

### Data Analysis

First, hemodynamic characteristics of “thin” and “atherosclerotic” blebs were compared using the non-parametric two-sample unpaired Wilcoxon (Mann Whitney) test. For this purpose, bleb hemodynamic variables were first normalized with their average value over the entire aneurysm. Bleb location with respect to the inflow stream were similarly compared but without normalization. The relationship between bleb location on the aneurysm sac and bleb wall type was analyzed using contingency tables and Pearson’s Chi-Squared test.

Secondly, blebs were subdivided by their location relative to the inflow (DINF, Supplementary Table II) into two groups: 1) “close” to inflow ( $DINF < 0.5$ ), and 2) “far” from inflow ( $DINF > 0.5$ ). Normalized hemodynamic characteristics of blebs close to and far from the inflow were then compared using the Wilcoxon test. Similarly, blebs were also subdivided by their location on the aneurysm neck, body, or dome region, and compared.

All statistical analyses were performed in R, and differences were considered significant if  $p < 0.05$ .

## Results

### Thin and Atherosclerotic Blebs

Average flow and location characteristics of “thin” and “atherosclerotic” blebs are presented and compared in Table 1. This corresponds to the subset of 32 aneurysms with 41 blebs visible in intra-operative videos (22 thin blebs, 19 atherosclerotic blebs). These results indicate that thin blebs tended to be located closer to the inflow (i.e. more aligned with the flow stream) than atherosclerotic blebs ( $p=0.0868$ ) and that maximum OSI tended to be larger in atherosclerotic blebs ( $p=0.0941$ ) but these associations were not significant.

In order to further explore these trends, a subset of aneurysms with multiple blebs of both kinds, thin and atherosclerotic ( $n=8$ ), was analyzed by computing the ratio of values of thin over atherosclerotic blebs of the same aneurysm, and compared them against one using one-sample Wilcoxon tests. This analysis (see Supplementary Table III) confirmed that thin blebs were located closer to the inflow (ratio DINF=0.53,  $p=0.0234$ ), and had lower OSI (ratio OSI=0.38,  $p=0.0156$ ) than atherosclerotic blebs of the same aneurysm. The WSS tended to be higher (ratio WSS=4.74,  $p=0.0781$ ) but this association was not significant. An illustrative example is presented in Fig. 2 (see further examples in Supplementary Figures I–II).

Additionally, Supplementary Table IV summarizes the number of ruptured and unruptured aneurysms with single or multiple blebs of different kinds visible in the intra-operative videos and the distribution of rupture sites in ruptured aneurysms with visible rupture points. Of the 12 ruptured aneurysms harboring blebs, 8 (67%) ruptured at a bleb, and 4 (33%) away from the blebs. Of the 8 that ruptured at a bleb, 5 (62%) ruptured at a thin bleb and 3 (38%) at an atherosclerotic bleb. Of 4 ruptured aneurysms with a single atherosclerotic bleb, the rupture point was at the bleb in 2 (50%) and away from the bleb in the other 2 (50%). In contrast, of the 5 ruptured aneurysms with a single thin bleb, 4 (80%) ruptured at the bleb, while only 1 (20%) away from the bleb. Of the 3 ruptured aneurysms with both thin and atherosclerotic blebs, 1 (33.33%) ruptured at the thin bleb, 1 (33.33%) at the atherosclerotic bleb, and 1 (33.33%) away from the blebs.

### Blebs at Different Locations

Hemodynamic characteristics of blebs located “close” (DINF<0.5) and “far” (DINF>0.5) from the inflow are presented in Table 2. Values of hemodynamic variables at regions of bleb formation (prior to their formation, obtained from simulations with the blebs virtually removed) are also given in this table. Note that in this part of the study, all 122 blebs were compared (not just those with blebs visible in the videos). On average, blebs close to the inflow had higher velocity (VEL,  $p=0.0213$ ), vorticity (VO,  $p=0.0057$ ), shear strain rate (SR,  $p=0.0084$ ), wall shear stress (WSS,  $p=0.0085$ ), WSS gradient (WSSGRAD,  $p=0.0151$ ), and WSS gradient oscillations (GON,  $p=0.0046$ ) than blebs far from the inflow. Prior to bleb

formation, similar significant differences were observed for WSS variables between regions of bleb formation close to and far from the inflow.

Similarly, hemodynamic characteristics of blebs located at the neck, body, or dome of the aneurysms are presented in Supplementary Table V. Pairwise comparisons indicate that blebs at the neck had larger distance to the inflow (DINF) than blebs at the body ( $p=0.0339$ ) or blebs at the dome ( $p=0.0032$ ). In addition, WSS gradient tended to be higher in blebs at the neck than in blebs at the dome ( $p=0.0567$ ), and it also tended to be higher in blebs at the body than in blebs at the dome ( $p=0.0522$ ), but these associations were only marginally significant.

## Discussion

The presence of blebs in IAs has been identified as a risk factor for aneurysm rupture in clinical studies.<sup>21–25</sup> Autopsy and surgical observations have also shown that aneurysm rupture sites tend to occur at blebs or in their immediate vicinity.<sup>26</sup> Hemodynamic studies have shown that low flow conditions characterized by low and oscillatory wall shear stress predominate within blebs.<sup>15,27</sup> Furthermore, blebs have been most commonly observed towards the dome of the aneurysms which typically tend to be under low flow conditions.<sup>1</sup> These observations have led to the common belief that blebs form in regions of slow recirculating flow and that aneurysms rupture at blebs because the low flow conditions predominant in blebs further promote wall degradation and weakening and the geometry of the bleb concentrates intramural stresses.<sup>28</sup> On the other hand, other studies have proposed that blebs could also form at or in the vicinity of flow impingement regions associated with localized elevations of the wall shear stress.<sup>14,29</sup> Moreover, a recent study suggested that blebs are more common in aneurysms exposed to flow conditions characterized by stronger flows and higher WSS compared to aneurysms where blebs did not form.<sup>19</sup> However, in all these previous studies, all blebs have been lumped together without distinguishing different kinds of blebs. Therefore, while the conclusions and observations of these previous studies as well as the common beliefs about blebs may be true for some blebs, they may not be true in general.

However, the main message of our report is that not all blebs are the same. In particular, our study has shown blebs with different wall characteristics as reflected in their visual appearance, i.e. thin translucent blebs seen red in videos, and atherosclerotic, usually thick walled, blebs seen white or yellow in videos. These different visual appearances are suggestive of different remodeling processes (or their impairment) that have led to distinct local wall structures. Furthermore, our study has identified blebs exposed to different hemodynamic environments, depending on their location relative to the inflow stream. Blebs near the inflow are exposed to higher flow conditions and larger spatial variations (gradients) compared to blebs far from the inflow, which tend to be exposed to more uniformly low flow conditions. In addition, our study found a trend of thin red blebs to be located closer to the inflow than white/yellow atherosclerotic blebs, suggesting that perhaps they evolve differently because they are exposed to different hemodynamic environments. Specifically, thin red blebs may form in regions exposed to strong flows, flow impingement, and large

WSS spatial gradients, while atherosclerotic blebs may form in regions of slow flow and low and oscillatory wall shear stress.

Our study also made interesting observations about the site of rupture of aneurysms harboring blebs (examples are presented in Supplementary Figures III–VI). In our database, approximately 52% of ruptured aneurysms had no blebs, while 48% harbored one or more blebs. Of the aneurysms harboring blebs, approximately 30% had multiple blebs. Approximately 80% of aneurysms with multiple blebs had blebs of both kinds (thin and atherosclerotic), while 20% had multiple thin blebs, and no aneurysm had multiple atherosclerotic blebs. In small subset of 12 ruptured aneurysms harboring blebs, the rupture site could be observed in intra-operative videos. These observations indicate wall failure and aneurysm rupture can happen both in thin and atherosclerotic blebs. Although the size of this sub-sample is too small for statistically significant conclusions, the data seems to suggest a slight tendency of thin red blebs to rupture more frequently than thick atherosclerotic blebs. Furthermore, in ruptured aneurysms harboring blebs failure away from the blebs is not rare (33% of cases).

The results and observations of our study suggest that different mechanisms of wall remodeling and degradation in response to locally high and low flow conditions may be at play simultaneously in cerebral aneurysms and may be responsible for the development and evolution of blebs with different wall structures. Both high and low flow conditions have been associated with detrimental effects on the walls of aneurysms<sup>30</sup>. We further speculate that perhaps co-existence of these adverse conditions and varying wall structures may be even more dangerous. Furthermore, diverse causes of failure may be related to the distinct local structure of bleb walls of different kinds and the transition between the bleb and the rest of the aneurysm sac. As such, perhaps there is no contradiction between studies proposing associations between low flow conditions and rupture and those proposing associations between high flow conditions and rupture. At any rate, the trends, conjectures, and hypotheses proposed in this study should be confirmed and further studied with larger datasets. Nevertheless, it is important to highlight the main message of this study which is that not all blebs are the same and their distinguishing characteristics should be taken into consideration when studying the mechanisms of wall degeneration and when evaluating aneurysms clinically to decide on immediate treatment or conservative observation.

## Conclusions

Not all blebs are equal; some have thin translucent walls while others have thick atherosclerotic walls. Thin blebs tend to be located closer to the inflow than atherosclerotic blebs. Blebs close to the inflow tend to be exposed to stronger flows with higher and spatially variable WSS than blebs far from the inflow that tend to have uniformly lower WSS. Aneurysms can rupture at thin blebs, at atherosclerotic blebs, as well as away from blebs. Further studies are needed to better understand wall failure in the presence of different kinds of blebs.

## Supplementary Material

Refer to Web version on PubMed Central for supplementary material.

## Funding

This work was supported by NIH grant R01NS097457.

## References

- Salimi Ashkezari S, Detmer F, Mut F, et al. Blebs in intracranial aneurysms: prevalence and general characteristics. *JNIS* 2020; DOI: 10.1136/neurointsurg-2020-016274.
- Lindgren AE, Koivisto T, Björkman J, et al. Irregular Shape of Intracranial Aneurysm Indicates Rupture Risk Irrespective of Size in a Population-Based Cohort. *Stroke* 2016;47:1219–26. [PubMed: 27073241]
- Greving JP, Wermer MJ, Brown RD, et al. Development of the PHASES score for prediction of risk of rupture of intracranial aneurysms: a pooled analysis of six prospective cohort studies. *Lancet Neurol* 2014;13:59–66. [PubMed: 24290159]
- Etminan N, Brown RD, Beseoglu K, et al. The unruptured intracranial aneurysm treatment score: a multidisciplinary consensus. *Neurology* 2015;85:881–9. [PubMed: 26276380]
- Backes D, Rinkel GJE, Greving JP, et al. ELAPSS score for prediction of risk of growth of unruptured intracranial aneurysms. *Neurology* 2017;88:1600–6. [PubMed: 28363976]
- Samaniego EA, Roa JA, Hasan D. Vessel wall imaging in intracranial aneurysms. *J Neurointerventional Surg* 2019;11:1105–12.
- Al Kasab S, Nakagawa D, Zanaty M, et al. In vitro accuracy and inter-observer reliability of CT angiography in detecting intracranial aneurysm enlargement. *J Neurointerventional Surg* 2019;11:1015–8.
- Hayakawa M, Katada K, Anno H, et al. CT Angiography with electrocardiographically gated reconstruction for visualizing pulsation of intracranial aneurysms: identification of aneurysmal protuberance presumably associated with wall thinning. *AJNR Am J Neuroradiol* 2005;26:1366–9. [PubMed: 15956499]
- Furukawa K, Ishida F, Tsuji M, et al. Hemodynamic characteristics of hyperplastic remodeling lesions in cerebral aneurysms. *PloS One* 2018;13:e0191287. [PubMed: 29338059]
- Cebral JR, Detmer F, Chung BJ, et al. Local Hemodynamic Conditions Associated with Focal Changes in the Intracranial Aneurysm Wall. *AJNR Am J Neuroradiol* 2019;40:510–6. [PubMed: 30733253]
- Robertson AM, Duan X, Hill MR, et al. Diversity in the strength and structure of unruptured cerebral aneurysms. *Ann Biomed Eng* 2014;43:1502–15.
- Gade PS, Tulamo R, Lee K-W, et al. Calcification in Human Intracranial Aneurysms Is Highly Prevalent and Displays Both Atherosclerotic and Nonatherosclerotic Types. *Arterioscler Thromb Vasc Biol* 2019;39:2157–67. [PubMed: 31462093]
- Frösen J, Cebral J, Robertson AM, et al. Flow-induced, inflammation-mediated arterial wall remodeling in the formation and progression of intracranial aneurysms. *Neurosurg Focus* 2019;47:E21.
- Cebral JR, Sheridan MJ, Putman CM. Hemodynamics and Bleb Formation in Intracranial Aneurysms. *AJNR Am J Neuroradiol* 2010;31:304–10. [PubMed: 19797790]
- Zhang Y, Mu S, Chen J, et al. Hemodynamic analysis of intracranial aneurysms with daughter blebs. *Eur Neurol* 2011;66:359–67. [PubMed: 22134355]
- Cebral JR, Castro MA, Appanaboyina S, et al. Efficient pipeline for image-based patient-specific analysis of cerebral aneurysm hemodynamics: Technique and sensitivity. *IEEE Trans Med Imag* 2005;24:457–67.
- Mut F, Aubry R, Löhner R, et al. Fast numerical solutions of patient-specific blood flows in 3D arterial systems. *Int J Num Meth Biomed Eng* 2010;26:73–85.



18. Durka MJ, Wong IH, Kallmes DF, et al. A data-driven approach for addressing the lack of flow waveform data in studies of cerebral arterial flow in older adults. *Physiol Meas* 2018;39:015006. [PubMed: 29205172]
19. Salimi Ashkezari S, Mut F, Chun BJ, et al. Hemodynamic Conditions that Favor Bleb Formation in Cerebral Aneurysms. *JNIS* 2020; DOI: 10.1136/neuriintsurg-2020-016369.
20. Mut F, Löhner R, Chien A, et al. Computational hemodynamics framework for the analysis of cerebral aneurysms. *Int J Num Meth Biomed Eng* 2011;27:822–39.
21. Beck J, Rohde S, el Beltagy M, et al. Difference in configuration of ruptured and unruptured intracranial aneurysms determined by biplanar digital subtraction angiography. *ACTA Neurochir* 2003;145:861–5. [PubMed: 14577007]
22. Sonobe M, Yamazaki T, Yonekura M, et al. Small unruptured intracranial aneurysm verification study: SUAVE study, Japan. *Stroke* 2010;41:1969–77. [PubMed: 20671254]
23. Morita A, Kirino T, Hashi K, et al. The natural course of unruptured cerebral aneurysms in a Japanese cohort. *N Engl J Med* 2012;366:2474–82. [PubMed: 22738097]
24. Burkhardt J-K, Fierstra J, Esposito G, et al. Rapid Documented Growth of Aneurysm Bleb Led to Rupture of an Incidental Intracranial Anterior Communicating Artery Aneurysm. *J Neurol Surg Part Cent Eur Neurosurg* 2017;78:521–4.
25. Yamano A, Yanaka K, Uemura K, et al. Bleb formation in small unruptured intracranial aneurysm as a predictor of early rupture. *J Surg Case Rep* 2018;2018:rjy117. [PubMed: 29977511]
26. Nyström SH. On factors related to growth and rupture of intracranial aneurysms. *Acta Neuropathol (Berl)* 1970;16:64–72. [PubMed: 5456388]
27. Kawaguchi T, Nishimura S, Kanamori M, et al. Distinctive flow pattern of wall shear stress and oscillatory shear index: similarity and dissimilarity in ruptured and unruptured cerebral aneurysm blebs. *J Neurosurg* 2012;117:774–80. [PubMed: 22920960]
28. Challa V, Han H-C. Spatial variations in wall thickness, material stiffness and initial shape affect wall stress and shape of intracranial aneurysms. *Neurol Res* 2007;29:569–77. [PubMed: 17535557]
29. Tateshima S, Murayama Y, Villablanca JP, et al. In vitro measurement of fluid-induced wall shear stress in unruptured cerebral aneurysms harboring blebs. *Stroke* 2003;34:187–92. [PubMed: 12511772]
30. Meng H, Tutino VM, Xiang J, et al. High WSS or Low WSS? Complex Interactions of Hemodynamics with Intracranial Aneurysm Initiation, Growth, and Rupture: Toward a Unifying Hypothesis. *AJNR Am J Neuroradiol* 2014;35:1254–62. [PubMed: 23598838]

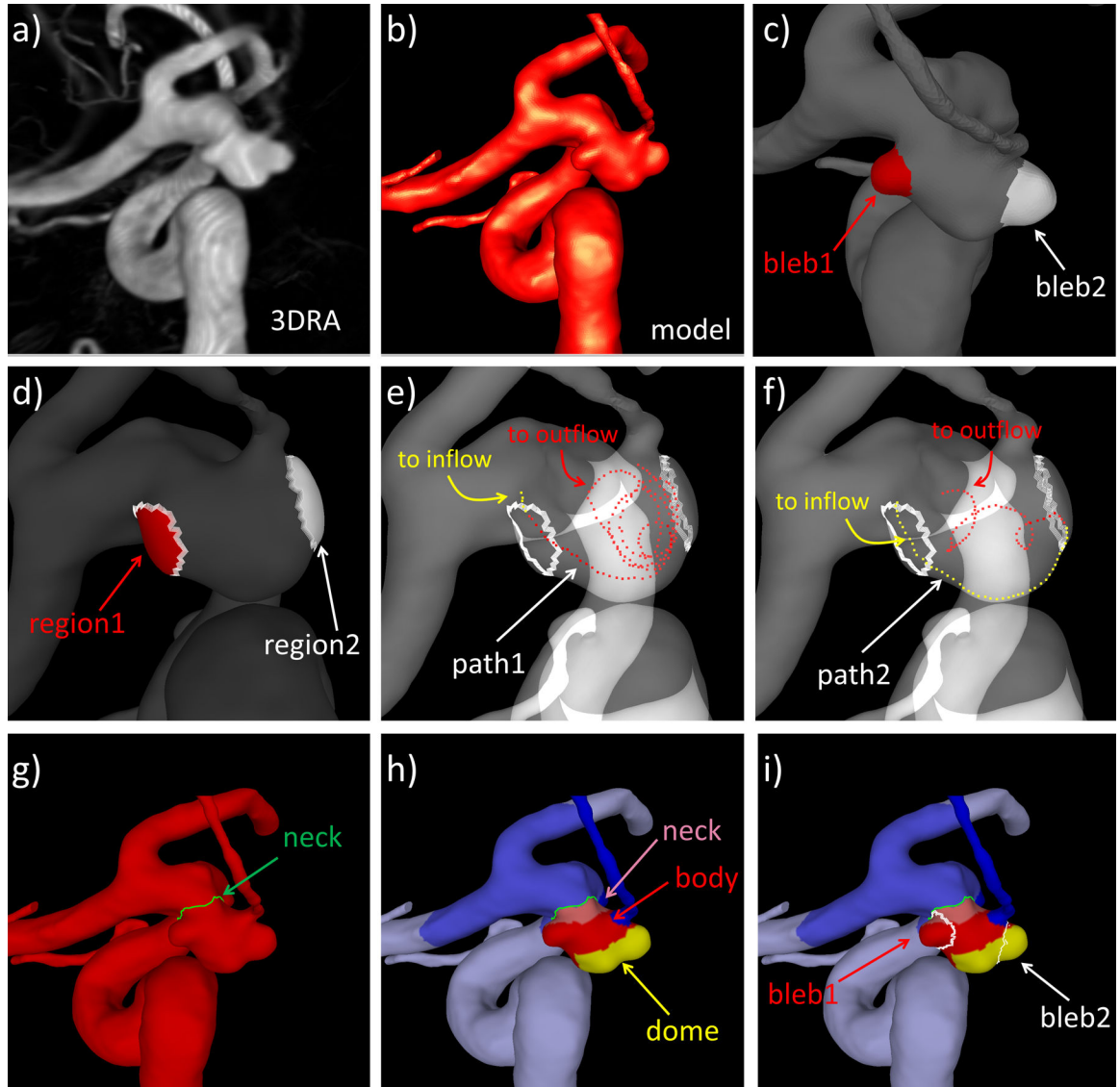


**Figure 1.**

Illustration of methodology: a) volume rendering of 3DRA image of aneurysm with two blebs, b) patient-specific vascular model reconstructed from 3DRA image, c) identification and marking of two blebs (bleb1=red, bleb2=white), d) automatic bleb removal and projection of bleb regions to model with deleted blebs, e) example streamline extending from inflow to seed near region1 (yellow dots) and from seed to outflow (red dots), f) example streamline extending from inflow to seed near region2 (yellow dots) and from seed to outflow (red dots), g) delineation of aneurysm neck, h) subdivision of aneurysm into neck (pink), body (red) and dome (yellow) regions, and i) bleb locations on aneurysm regions.

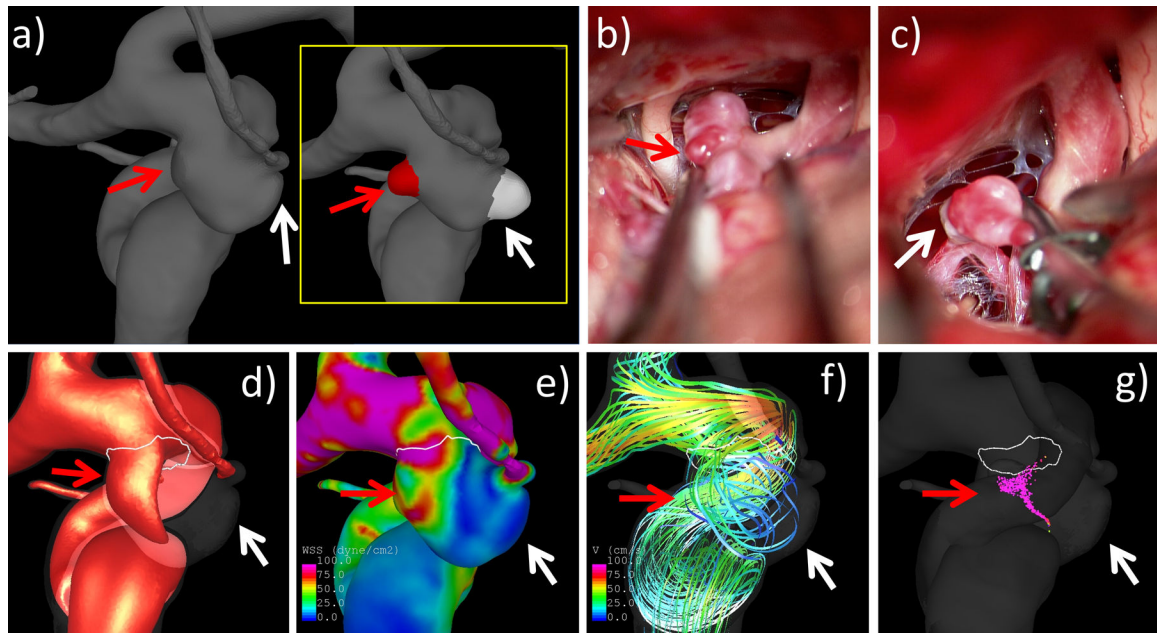


**Figure 2.**

Example of analysis of an aneurysm with a thin bleb (red) and an atherosclerotic/hyperplastic (white) bleb: a) anatomical model with blebs removed (insert shows the two marked blebs prior to virtual removal), b) thin red bleb (red arrow) observed in intra-operative video, c) hyperplastic/atherosclerotic white bleb (white arrow) in video, d) visualization inflow stream, e) WSS distribution, f) flow pattern visualized with streamlines, and g) flow structure visualized with vortex corelines. All flow visualizations correspond to peak systole. Arrows point to the regions of each bleb formation. Note that the red bleb is located closer to the inflow than the white bleb.

**Table 1.**

Comparison of (normalized) hemodynamic characteristics (prior to virtual bleb removal) and locations of thin (red) blebs and atherosclerotic (white/yellow) blebs. Values are given as mean  $\pm$  standard deviation.

Characteristic	Variable	Bleb Wall Type		P-value
		Thin Red	Atherosclerotic White/Yellow	
Flow Strength	VEL	0.455 $\pm$ 0.410	0.362 $\pm$ 0.414	0.3572
	VO	0.890 $\pm$ 0.635	0.572 $\pm$ 0.541	0.1481
	SR	1.024 $\pm$ 0.715	0.648 $\pm$ 0.570	0.1271
WSS Distribution	WSS	0.630 $\pm$ 0.469	0.474 $\pm$ 0.544	0.1557
	OSI(max)	0.375 $\pm$ 0.325	0.541 $\pm$ 0.296	0.0941
	RRT	1.839 $\pm$ 1.639	2.451 $\pm$ 1.417	0.1026
	WSSGRAD	0.934 $\pm$ 0.650	0.662 $\pm$ 0.400	0.1801
	GON	0.999 $\pm$ 0.543	0.923 $\pm$ 0.406	0.6321
Bleb Location	DINF	45.64 $\pm$ 22.31	58.40 $\pm$ 16.81	0.0868
	Dome	8	14	0.3759
	Body	10	7	
	Neck	1	1	

**Table 2.**

Comparison of (normalized) hemodynamic characteristics between blebs close to the inflow and blebs far from the inflow (after bleb development), and between regions of bleb development (before bleb formation) located close to or far from the inflow.

Simulation	Variable	Location relative to inflow		P-value
		Close	Far	
After Bleb Development (before virtual removal)	VEL	0.467 ± 0.387	0.316 ± 0.295	0.0213*
	VO	0.830 ± 0.577	0.571 ± 0.463	0.0057*
	SR	0.944 ± 0.635	0.668 ± 0.512	0.0084*
	WSS	0.610 ± 0.460	0.424 ± 0.373	0.0085*
	OSI(max)	0.559 ± 0.312	0.448 ± 0.336	0.0643
	RRT	1.974 ± 1.622	2.708 ± 2.636	0.0725
	WSSGRAD	0.829 ± 0.533	0.622 ± 0.458	0.0151*
	GON	1.088 ± 0.519	0.805 ± 0.423	0.0046*
Before Bleb Formation (after virtual removal)	WSS	0.731 ± 0.504	0.543 ± 0.401	0.0209*
	OSI(max)	1.436 ± 1.305	1.047 ± 1.293	0.0314*
	RRT	1.361 ± 0.934	1.612 ± 1.310	0.4483
	WSSGRAD	0.679 ± 0.425	0.496 ± 0.385	0.0031*
	GON	1.079 ± 0.684	0.823 ± 0.557	0.0255*

Values are given as mean ± standard deviation. Significant differences (95% confidence,  $p < 0.05$ ) are marked with a “\*”.